

Photocurrent and capacitance spectroscopy of Schottky barrier structures incorporating InAs/GaAs quantum dots

P. N. Brunkov,* A. Patanè, A. Levin, L. Eaves, and P. C. Main

School of Physics and Astronomy, University of Nottingham, NG7 2RD Nottingham, United Kingdom

Yu. G. Musikhin, B. V. Volovik, A. E. Zhukov, V. M. Ustinov, and S. G. Konnikov
A. F. Ioffe Physico-Technical Institute, Polytechnicheskaya 26, 194021 St. Petersburg, Russia

(Received 29 March 2001; revised manuscript received 31 August 2001; published 8 February 2002)

We present photocurrent, capacitance, and photoluminescence studies of GaAs-based Schottky barrier structures incorporating InAs self-assembled quantum dots. We show that the photocurrent is mainly controlled by thermal escape of electrons out of the dots and is suppressed at low temperatures, below 100 K. At higher temperatures (>185 K), we are able to control the magnitude of the photon absorption, and hence the photocurrent, by varying the bias voltage applied to the device.

DOI: 10.1103/PhysRevB.65.085326

PACS number(s): 78.67.Hc, 73.63.Kv, 73.40.Qv

I. INTRODUCTION

InAs/GaAs self-assembled quantum dots (QD's) are of great current interest. Their zero-dimensional character has potential for new optoelectronic devices, such as low-threshold lasers¹ infrared detectors,^{1,2} and high-density optical memories.^{3,4} Carrier transport plays an important role in determining the properties of these devices. Therefore, a great deal of attention has been devoted to studies of emission and capture processes of charge carriers by the QD's using both electrical⁵⁻⁹ and optical techniques.¹⁰⁻¹³ Capacitance-voltage $C(V)$ measurements provide information about the electronic structure of the QD's;⁵⁻⁷ carrier escape processes from the QD's can be investigated by time-resolved capacitance measurements, which can separate thermionic and tunneling escape mechanisms.^{8,9} In addition, photocurrent (PC) spectroscopy combines the advantages of both electrical and optical methods of investigation.¹¹⁻¹³ The PC spectrum reflects, in part, the optical absorption in the QD layer, but carriers that are photogenerated in the QD's have to be separated in order to contribute to the PC signal. As a result, the intensity of the PC signal is governed by the interplay between the recombination and escape rates of photogenerated carriers.¹¹

Previous work on PC spectroscopy¹¹⁻¹³ has principally involved $p-i-n$ structures, in which the QD layers were placed in the high electric field of the intrinsic i layer. In this type of structure, the QD's are empty and it is not possible to determine the electronic structure and the escape parameters of the QD's using capacitance spectroscopy. Chang *et al.*¹³ have found that the temperature dependence of the PC signal from InAs QD's is controlled by thermally assisted hole tunneling, implying that holes are the more weakly confined carriers. However, capacitance spectroscopy measurements on InAs QD's indicate that the hole ground state may have a larger binding energy than the corresponding electron level, relative to the corresponding band edge.⁶ In addition, time-resolved capacitance spectroscopy has revealed that the hole escape rate from the QD's is much lower than the electron escape rate.⁹ To resolve this apparent contradiction, it is necessary to use both capacitance and PC spectroscopy to pro-

vide a complete description of the electronic properties of a QD structure. In this paper, we report both capacitance and PC spectroscopy of a Schottky barrier structure, incorporating InAs QD's in a uniformly doped n -GaAs layer. The analysis of photoluminescence (PL) and $C(V)$ measurements allows us to determine the electronic structure of the QD's and the escape rate of carriers out of the dots. The results obtained are then used in the analysis of the PC data. We also show that it is possible to control the photon absorption in QD's by changing their electron occupation. In principle, it is therefore possible to use the bias to modulate the QD absorption.

The paper is organized as follows. In the following section, we describe the growth conditions and compositional structure of our sample. In Sec. III, we investigate the electronic structure of the dots using PL and $C(V)$ measurements. In Sec. IV, we use admittance spectroscopy to investigate the thermal escape of electrons from the dots. In combination with PL and $C(V)$ studies, this allows us to identify the mechanisms responsible for the PC signal due to QD's. The paper concludes with a summary (Sec. V).

II. SAMPLES

The QD structure was grown by molecular-beam epitaxy on a n^+ -GaAs (001) substrate. The InAs layer, of average thickness 4 monolayers, was deposited at 485 °C. The QDs were sandwiched between a 0.4- μm -thick GaAs cap and a 1- μm -thick GaAs buffer layer. The cap and buffer layers were uniformly doped with Si at $2 \times 10^{16} \text{ cm}^{-3}$, except for two 10 nm thick, undoped spacers, one on each side of the QD layer [see Fig. 1(a)]. Plan-view transmission electron-microscopy images reveal a uniform spatial distribution of dots, with mean diameter of 15 nm. The areal concentration was found to be $N_{\text{QD}} = (3.5 \pm 0.5) \times 10^{14} \text{ m}^{-2}$.

A Ni-Cr Schottky barrier of 350 μm diameter was deposited on top of the n -type structure for capacitance and conductance, G , measurements. The $C(V)$ and $G(V)$ characteristics were measured using an HP4275A or an HP4284A LCR meter. For the PC and PL measurements, a semitransparent, Ni-Cr Schottky barrier of diameter 100 μm was de-

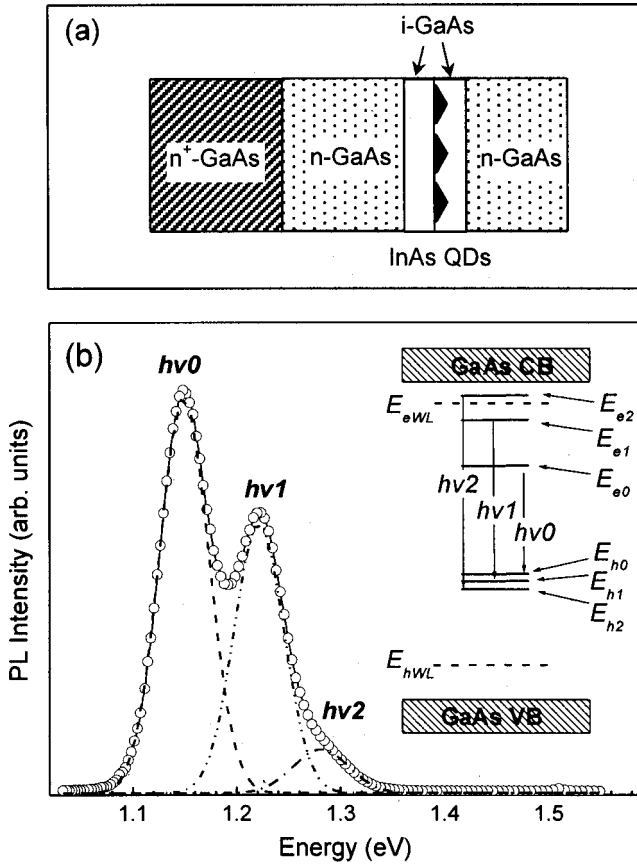


FIG. 1. (a) Sketch of the sample structure. (b) Photoluminescence (PL) spectrum of InAs/GaAs self-assembled quantum dots measured at $T=80$ K with 20 W/cm^2 excitation power. The continuous line is a fit to the data using three Gaussians. The inset sketches the electronic structure of the dots.

posited on top of the structure to provide optical access to the sample. The excitation source for the PC measurements was a tungsten-halogen lamp, dispersed by a 0.25 m monochromator and the PC signal was recorded using standard lock-in techniques. PL measurements were performed with the optical excitation provided by a He-Ne laser.

III. ELECTRONIC STRUCTURE OF QD's

Figure 1(b) shows the PL spectrum of the QD structure at $T=80$ K. We observe three QD-related bands, $h\nu0$, $h\nu1$, and $h\nu2$ peaked, respectively, at 1.150, 1.222, and 1.281 eV. Band $h\nu0$ is due to ground-state electron-hole transitions in the dots, whilst $h\nu1$ and $h\nu2$ are due to transitions involving the excited-electron and hole states.^{14,15} Each PL band has a linewidth of $\Delta E \approx 50$ meV, obtained by fitting the measured spectrum to three Gaussian curves. Increasing the power increases the intensity of the high energy bands relative to that of the ground-state peak $h\nu0$. Also, increasing the temperature tends to suppress the PL peaks, due to the thermal escape of carriers from the QD's.

Model calculations of the energy levels of InAs/GaAs QD's, similar to those considered in the present work, indi-

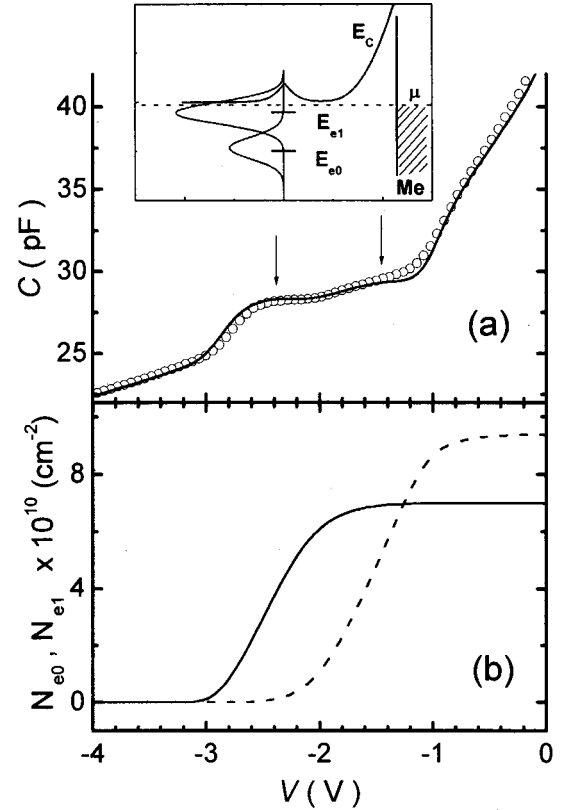


FIG. 2. (a) Capacitance-voltage characteristic $C(V)$ measured at 1 kHz and $T=80$ K (open circles), simulated using a quasistatic model (continuous line). The inset shows the conduction band diagram of the QD structure at zero bias. The horizontal lines represent the mean energies E_{ei} of the QD levels. (b) Occupation of the electron ground (solid line) and first excited (dashed line) state in QD's as a function of the reverse bias as determined from the simulation of the $C(V)$ data.

cate that the energy separation of hole states in the dots is only a few meV (<11 meV).¹⁴ This implies that the large-energy spacing $\Delta E > 60$ meV between bands $h\nu0$, $h\nu1$, and $h\nu2$ is mainly due to the energy separation ΔE_e between successive electron states of the dot. In particular, the energy spacing between bands $h\nu0$ and $h\nu1$ ($\Delta E=72$ meV) is within the range of values of the energy splitting $\Delta E_{e0-1} = 70-90$ meV between the ground state and the first excited state of the electron calculated in Ref. 14.

We investigated in further detail the electron states of the dot by means of $C(V)$ measurements. As shown in Fig. 2(a), the $C(V)$ characteristic of the QD structure shows two plateau regions indicated by arrows, with a small step between them at -2.0 V, indicating the filling of two electronic states of the QD's.⁷ At a given temperature, the charge located in the QD plane is determined by the sheet concentration N_{QD} of the QD's and by the positions of the electron energy levels in the QD's, E_{ei} , relative to the chemical potential μ [see inset in Fig. 2(a)]. We use a Gaussian distribution to describe the density of states associated with the distribution of QD sizes. The density of charge Q_{QD} accumulated in the QD plane may be written as^{6,7}

$$Q_{\text{QD}} = e \sum_i \int \sqrt{\frac{2}{\pi}} \frac{g_i N_{\text{QD}}}{\Delta E} \times \exp[-2(E - E_{ei})^2 / \Delta E^2] f(E, \mu) dE, \quad (1)$$

where $f(E, \mu)$ is the Fermi function, g_i is the spin-degeneracy factor, and e is the electron charge. The summation ($i=0,1,2$) is taken over all dot energy levels.

A quasistatic charging model⁶ is used to fit the $C(V)$ curve at $T=80$ K, as shown in Fig. 2(a). The numerical analysis indicates that, at $V=0$ V, there are two filled electron states in the QD's, at $E_{e0}=(140 \pm 10)$ meV and $E_{e1}=(60 \pm 10)$ meV below the bottom of the GaAs conduction band [see the inset in Fig. 2(a)] both with width $\Delta E=(50 \pm 10)$ meV deduced independently from the PL measurements. We believe that, due to the band-bending effects caused by the charging of the dots, the highest energy states of the dot are empty and cannot be measured by $C(V)$ (see inset of Fig. 2). However, the observation of the QD-related band $h\nu 2$ in the PL indicates the existence of a second electron excited state in the dot.

The first two electron energy levels derived from $C(V)$ measurements, $E_{e0}=(140 \pm 10)$ meV and $E_{e1}=(60 \pm 10)$ meV, are close to the values calculated for {113} faceted dots ($E_{e0}=177$ meV and $E_{e1}=86$ meV).¹⁴ The same model predicts a second electron energy level $E_{e2}=77$ meV and an energy spacing between E_{e1} and E_{e2} , $\Delta E_{e1-2}=9$ meV. If we assume that band $h\nu 2$ is due to a transition from the second excited states to the holes states, then the large-energy spacing of 60 meV between bands $h\nu 1$ and $h\nu 2$ is not consistent with ΔE_{e1-2} . However, this inconsistency may be due to the different shape and compositional profile of the dot assumed in the model compared to the actual dots in our experiment. Also, the measured value of $E_{e1}=(60 \pm 10)$ meV and the calculated electron energy level $E_{e\text{WL}}=30\text{--}50$ meV of the InAs wetting layer (WL), suggest that the second excited state has a small binding energy [see inset of Fig. 1(b)] or is possibly in resonance with the levels of the WL continuum states.

The $C(V)$ measurements indicate that the energy splitting ΔE_{e0-1} between the ground state and the first excited state of the electron in the dot is $\Delta E_{e0-1}=80 \pm 20$ meV. This value is comparable with the energy spacing of bands $h\nu 0$ and $h\nu 1$ derived from the PL measurements $\Delta E \sim 70$ meV and is within the range of values of $\Delta E_{e0-1}=70\text{--}90$ meV calculated in Ref. 14.

The comparative analysis of the PL and the $C(V)$ measurements allows us to determine the hole energy levels. As sketched in the inset of Fig. 1(b), the sum of the ground-state electron energy $E_{e0}=140$ meV, the ground-state hole energy E_{h0} , and the ground-state recombination energy $h\nu 0=1150$ meV should correspond to the GaAs band gap at 80 K, $E_{\text{GaAs}} \sim 1507$ meV. Hence, we estimate the position of the hole ground-state level in the QD's to be $E_{h0}=(200 \pm 10)$ meV above the top of the GaAs valence band. This estimate includes a small correction due to the exciton binding energy in the QD's, which is ~ 20 meV.¹ A similar analysis for the first hole excited state gives $E_{h1}=205 \pm 10$ meV, a value that is very close to E_{h0} , thus supporting the prediction

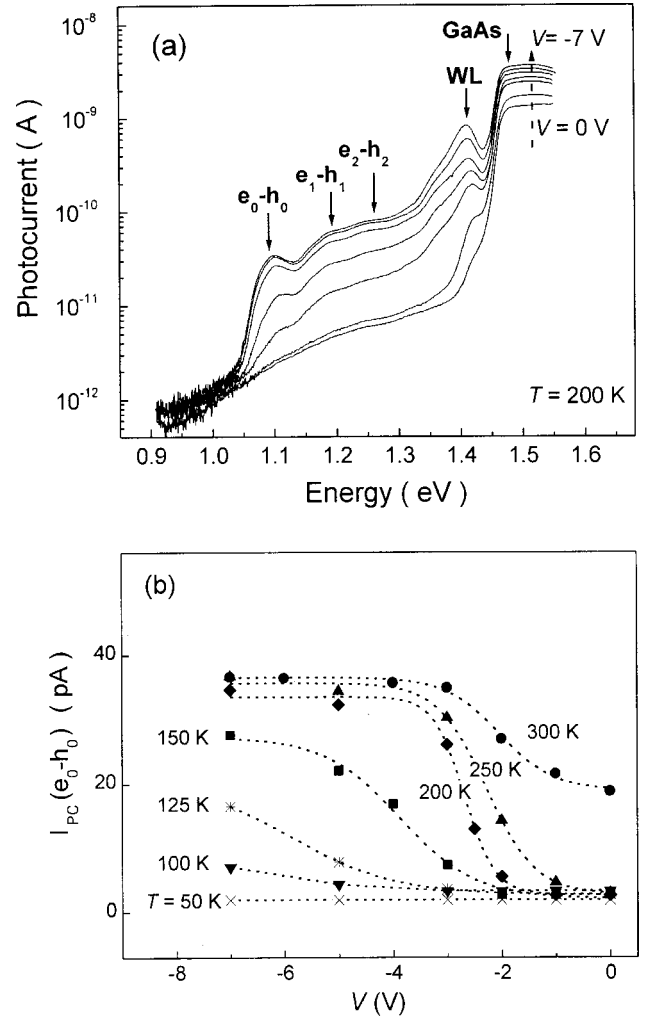


FIG. 3. (a) Photocurrent (PC) spectra measured as a function of reverse bias V at $T=200$ K. From the bottom to the top, V is equal to 0, -1 , -2 , -2.5 , -3 , -5 , -7 V. (b) Intensity of the PC ground-state peak $I_{\text{PC}}(e_0-h_0)$ versus V at various temperatures.

of a small energy separation between the two first hole levels of QD's (~ 7 meV),¹⁴ which is within the error of our measurement (~ 10 meV).

IV. PHOTOCURRENT SPECTROSCOPY OF QD's

Figure 3(a) shows logarithmic PC spectra of the device measured at $T=200$ K for various reverse biases. At $V=0$ V, the PC spectrum is dominated by a step at 1.45 eV related to the absorption by bulk GaAs. An increase of the reverse bias up to -7 V leads to the appearance of features at ~ 1.40 eV, due to optical absorption in the InAs wetting layer, and three features at 1.102, 1.182, and 1.240 eV, caused by absorption into the ground and excited states of the InAs QD's. The positions of the last three features agree quite well with the energy positions of the corresponding PL peaks measured at 200 K, taking into account a small Stokes shift (<10 meV) related to carrier thermalization.¹⁶

As shown in Fig. 3(a), the PC signal from the QD's measured at $T=200$ K grows monotonically with increasing re-

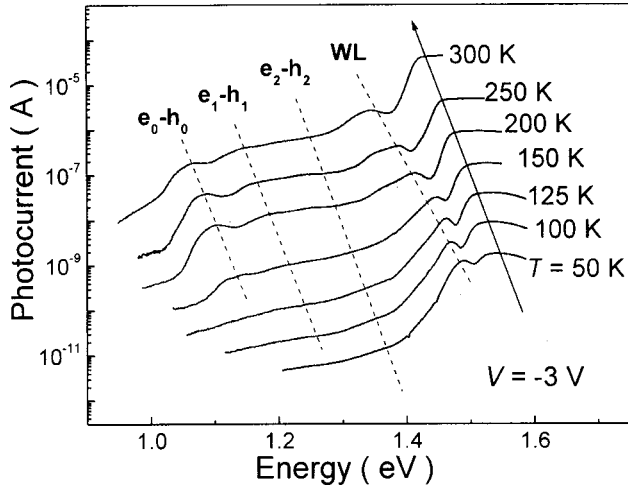


FIG. 4. (a) Photocurrent (PC) spectra measured for $V = -3$ V at various temperatures. The current scale applies to the lowest curve. For clarity, the different curves are displaced along the vertical axis.

verse bias, almost saturating at $|V| > 3$ V. Similar behavior is observed in the temperature range from 180 to 300 K [see Fig. 3(b)]. Below 180 K, the voltage modulation of the PC signal becomes weaker and, below 100 K, there is no PC signal from the QD's. The temperature dependence of the PC spectra measured at reverse bias $V = -3$ V shows that the PC signal from QD's is suppressed below 200 K, as shown in Fig. 4.

Analysis of the $C(V)$ characteristics indicates that, at $V = 0$ V, the two lowest electron states of the QD's are filled with electrons. This is shown in Fig. 2(b), which plots the occupation of electron ground and first excited state in the QD's as a function of the reverse bias, as determined by a simulation of the $C(V)$ characteristic. Increasing the magnitude of the reverse bias from 0 to -3 V results in successive depopulation of the levels E_{e1} and E_{e0} , respectively. Note that the PC signal from the QD states increases over this voltage range [Fig. 3(b)]. It is found from $C(V)$ measurements that at $|V| > 3$ V, there are no electrons occupying the ground-state level in the QD's [Fig. 2(b)]. Note that this value of the reverse bias agrees very well with the onset of the saturation of the PC signal from the QD's [Fig. 3(b)]. This suggests that the reason for the absence of the PC signal at low bias is that no absorption is possible because most of the dots are occupied. Thus, by changing the electron occupation in the QD's, one can use the reverse bias to control the photon absorption and, consequently, the PC signal. At 300 K, the voltage modulation of the PC signal from the QD's is weaker [Fig. 3(b)] because the concentration of electrons in the ground state of the QD's decreases with increasing temperature so that a PC signal is observed even at $V = 0$ V.

The amplitude of the PC signal from the QD's depends on the photon absorption. However, carriers photogenerated in the QD's can recombine before they are able to escape and contribute to the PC signal.^{11–13} Therefore, the strength of PC signal from the dots depends also on the relation between the recombination ($1/\tau_{\text{rec}}$) and escape rates ($1/\tau_{\text{esc}}$) of carriers. In particular, as follows from a coupled-rate equation

model, the intensity of the PC signal is mainly controlled by the escape rate of the faster carrier and can be represented in the following form^{13,17}

$$I_{\text{PC}} = \frac{g}{\left(1 + \frac{\tau_{\text{esc}}}{\tau_{\text{rec}}}\right)} \quad (2)$$

where g is the carrier photogeneration rate in the QD's, which is proportional to the incident photon flux P . Then, since the electron-hole recombination time is about 1 ns,¹⁰ for significant PC, τ_{esc} should be smaller than 1 ns.

The electron escape time can be expressed as

$$\tau_{\text{esc}}^e = \tau_{\text{esc}}^0 \exp(\Delta E_a^{e0}/kT). \quad (3)$$

where ΔE_a^{e0} is the activation energy for thermal escape of carriers and τ_{esc}^0 is the escape time in the high-temperature limit $kT \gg \Delta E_a^{e0}$. A similar expression holds also for the hole time constant.

In order to measure the temperature dependence of the electron escape rate out of the dots, we used admittance spectroscopy. Admittance spectroscopy involves measuring the capacitance and conductance of the device in the ac mode with tunable frequency f . As discussed in Ref. 7 and 18, a step in the $C(V)$ curve and a peak in the $G(V)$ characteristic of the device are observed when the rate of escape of electrons $1/\tau_{\text{esc}}^e$ out of the dots becomes comparable with f , according to the relation

$$2\pi f \tau_{\text{esc}}^e \cong 2. \quad (4)$$

At a fixed frequency, as the temperature decreases, $1/\tau_{\text{esc}}^e$ becomes lower than πf , i.e., carriers freeze into the QD states. This reveals itself as a characteristic T dependence of the capacitance and conductance curves: with increasing T , the capacitance shows a steplike behavior and the conductance exhibits a peak as shown in Fig. 5(a,b). The analysis of the $C(T)$ and $G(T)$ curves measured at different frequencies allow us to determine the temperature dependence of τ_{esc}^e .⁷ In particular, using admittance spectroscopy in the range of the reverse biases from -2.1 to -3.0 V, we can measure τ_{esc}^e associated with thermal escape of electrons from the ground state of the QD's: by changing V , we are able to vary the position of the electron levels in the QD's, E_{ei} , relative to the chemical potential μ [see inset in Fig. 2(a)]. As indicated by the quasistatic $C(V)$ simulations [Fig. 2(a, b)], depopulation of the electron ground state of the QD's occurs in the range of the reverse biases V from -2 to -3 V.

Figure 5(c) shows the Arrhenius plot of τ_{esc}^e and a fit to the data by Eq. (3), with fitting parameters ΔE_a^{e0} and τ_{esc}^0 listed in Table I. In the range of bias, -2.3 to -2.9 V, we find that ΔE_a^{e0} varies in the range 64–107 meV. We attribute this spread of values to the energy distribution of the dots caused by fluctuations in their size, composition, and shape. In particular, we find that at $V = -2.4$ V, the chemical potential μ is in resonance with the maximum of the density of states associated with the ground-state energy distribution of QD's [see inset of Fig. 2(a)]. For this bias condition, the

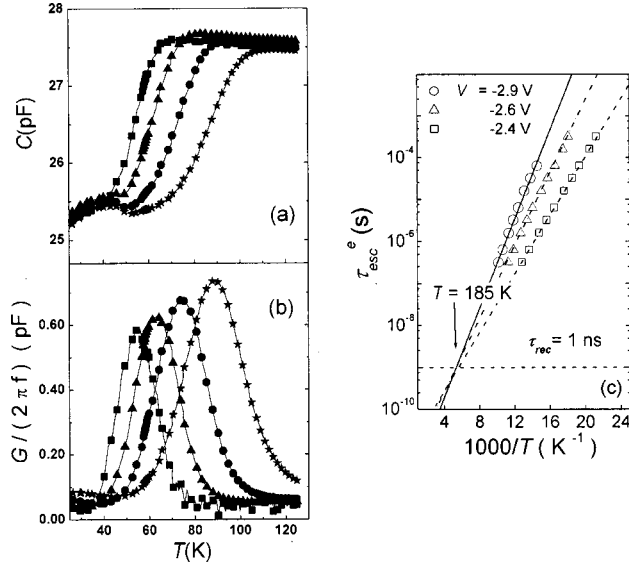


FIG. 5. Temperature dependence of (a) capacitance, C , and (b) conductance, G , measured at $V = -2.6$ V as a function of the measurement frequency f : 1 kHz (solid squares), 10 kHz (solid triangles), 100 kHz (solid circles), 1000 kHz (solid stars). (c) Arrhenius plots of the electron emission rate at different reverse biases. Continuous lines are fits to the data by Eq. (3).

value of ΔE_a^{e0} is equal to 69 meV. This quantity is smaller than the energy of the electron ground state $E_{e0} = 140$ meV determined from the quasistatic $C(V)$ simulations [Fig. 2(a)] and compares with the spacing between the ground state and first excited state of electrons in the QD's, $\Delta E_e = 80 \pm 20$ meV, as obtained from $C(V)$ measurements. This suggests that electron emission from the QD's into the GaAs layers occurs by thermal escape of electrons out of excited states of the dots. This is in agreement with the results obtained by time-resolved capacitance spectroscopy.^{9,19}

We can now interpret the observed temperature dependence of the PC signal in terms of our analysis of all the measurements. Figures 6(a) show the temperature dependence of the intensity of the PC peak associated with the QD ground state $I_{\text{PC}}(e_0 - h_0)$ at $V = -3.0$ V. The temperature dependence of the PC signal is well described by Eq. (2) and (3), using electron-escape parameters ΔE_a^{e0} and τ_{esc}^0 measured by admittance spectroscopy in the voltage range -2.3 – -2.9 V (Table I). For $V < -2.9$ V, we are not able to measure electron-escape rate by admittance spectroscopy be-

TABLE I. Values of ΔE_a^{e0} and τ_{esc}^0 determined from the Arrhenius plots of Fig. 5.

V (V)	τ_{esc}^0 (ps)	ΔE_a^{e0} (meV)
-2.3	11.3	64
-2.4	10.9	69
-2.5	8.8	76
-2.6	4.8	86
-2.8	1.1	100
-2.9	1.1	107

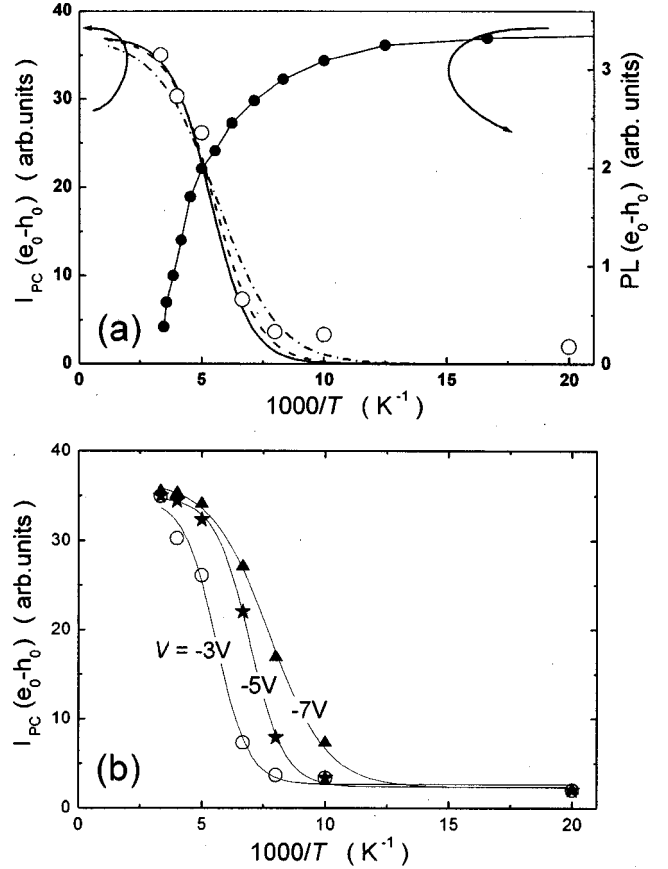


FIG. 6. (a) Temperature dependence of the intensity of the PC peak $I_{\text{PC}}(e_0 - h_0)$ for $V = -3$ V (open circles) and of the PL peak, $\text{PL}(e_0 - h_0)$, (solid circles) associated with the ground-state transition in the QD's. The calculated temperature dependence of $I_{\text{PC}}(e_0 - h_0)$ for thermal escape of electrons from QD's at different reverse biases are also shown: $V = -2.4$ V (dash-dotted line), -2.6 V (dotted line), -2.9 V (solid line). (b) Temperature dependence of $I_{\text{PC}}(e_0 - h_0)$ at different V . Continuous lines are guides to the eye.

cause the dots are not filled with electrons. A good agreement between the model and the data is obtained for V in the range -2.4 – -2.9 V [see Fig. 6(a)]. This indicates that the strength of the PC signal is determined by the electron-escape rate. For the holes, previous measurements⁹ in p doped devices incorporating QD's similar to that considered in this work, showed that the thermal activation of holes from the QD ground state has an activation energy of $\Delta E_a^{h0} = (164 \pm 10)$ meV. The value of ΔE_a^{h0} is smaller than the position of the hole ground-state level in the QD's measured by our $C(V)$ measurements $E_{h0} = (200 \pm 10)$ meV and suggests that the thermal activation of holes involves both the ground and the higher excited states of the dots, which are separated by only few meV (see discussion of Sec. III). Since the holes are heavier and more deeply confined than the electrons, if tunneling is involved in the escape process, their transmission coefficient should be lower. Therefore, in modeling the PC data, we can assume that the escape rate $(\tau_{\text{esc}}^e)^{-1}$ of photoexcited electrons from the QD's is a few orders of magnitude larger than the hole escape rate $(\tau_{\text{esc}}^h)^{-1}$. In this case, the photocurrent is proportional to $(\tau_{\text{esc}}^e)^{-1}$ at sufficiently

low temperature when $\tau_{\text{esc}}^e \gg \tau_{\text{rec}}$ [Eq. (2)]. At high temperatures, when the electron-escape rate is very high, the current is independent of τ_{esc}^e (and τ_{esc}^h) and is determined simply by the rate of photon absorption by the QD's [Eq. (2)].

Under the conditions of our experiment, the incident photon flux is relatively low: the strength of the PC signal increases linearly with photon flux P , with no indication of saturation of the QD absorption. Therefore, most of the QD's remain unexcited and neutral so that the positive charging of the QD's by the higher electron-escape rate has a negligible effect on the dynamics of the carrier escape from the QD's.

Figure 6(a) shows that for $T < 110$ K there is a strong increase in the intensity of the PL peak, $\text{PL}(e_0 - h_0)$, associated with the ground-state transition in the QD's. This implies that, in this temperature range, the recombination of photogenerated carriers dominates over escape processes, consistent with our description of the thermally activated PC associated with the QD's. In particular, we estimate that the electron escape time constant is lower than the recombination time $\tau_{\text{rec}} = 1$ ns for temperatures $T > 185$ K [Fig. 5(c)], consistent with the experimentally observed suppression of the PC signal from the QD's measured at $V = -3.0$ V [Fig. 4(a)].

Figure 6(b) shows the temperature dependence of the PC signal for different applied biases. Varying V from -3 to -7 V results into a weaker T dependence of the PC signal. In particular, for $V = -7$ V the PC signal becomes almost zero

for $T < 145$ K, while for $V = -2$ V, it quenches for $T < 185$ K. This behavior is due to the increasing rate of tunneling escape of electrons out of the dots with increasing bias.^{11,12,20} In our structure, the main contribution to the PC signal is due to thermally activated tunneling of electrons out of the dots. The maximum value of the electric field used in our experiments is 100 kV/cm, which is not enough to recover the PC signal by simple tunneling processes at the lowest temperatures (< 100 K).

V. CONCLUSIONS

In summary, we have shown that it is possible to control photon absorption in QD's by changing their electron occupation by means of an applied bias. In principle, it is therefore possible to use the reverse bias to modulate the optical absorption of a QD array. In addition, we have found that the temperature dependence of the PC signal from the QD's is governed by the relatively fast thermal escape of electrons.

ACKNOWLEDGMENTS

The work is supported by the Russian Ministry of Sciences project on nanoelectronics and by EPSRC. P.N.B. gratefully acknowledges support from the Royal Society. The authors would like to thank Dr. P. Dawson (U.M.I.S.T.) for fruitful discussion regarding this work.

*Permanent address: A. F. Ioffe Physico-Technical Institute, Polytechnicheskaya 26, 194021 St. Petersburg, Russia.

¹D. Bimberg, M. Grundmann, and N. N. Ledentsov, *Quantum Dot Heterostructures* (Wiley, Chichester, 1998).

²L. Chu, A. Zrenner, G. Böhm, and G. Abstreiter, *Appl. Phys. Lett.* **75**, 3599 (1999).

³S. Muto, *Jpn. J. Appl. Phys.* **34**, 210 (1995).

⁴Y. Sugiyama, Y. Nakata, S. Muto, Y. Awano, and N. Yokoyama, *Physica E (Amsterdam)* **7**, 503 (2000).

⁵G. Medeiros-Ribeiro, D. Leonard, and P. M. Petroff, *Appl. Phys. Lett.* **66**, 1767 (1995).

⁶P. N. Brunkov, A. Polimeni, S. T. Stoddart, M. Henini, L. Eaves, P. C. Main, A. R. Kovsh, Y. G. Musikhin, and S. G. Konnikov, *Appl. Phys. Lett.* **73**, 1092 (1998).

⁷P. N. Brunkov, A. R. Kovsh, V. M. Ustinov, Y. G. Musikhin, N. N. Ledentsov, S. G. Konnikov, A. Polimeni, A. Patanè, P. C. Main, L. Eaves, and C. M. A. Kapteyn, *J. Electron. Mater.* **28**, 486 (1999).

⁸S. Anand, N. Carlsson, M. E. Pistol, L. Samuelson, and W. Seifert, *Appl. Phys. Lett.* **67**, 3016 (1995).

⁹C. M. A. Kapteyn, M. Lion, R. Heitz, D. Bimberg, P. N. Brunkov, B. V. Volovik, S. G. Konnikov, A. R. Kovsh, and V. M. Ustinov, *Appl. Phys. Lett.* **76**, 1573 (2000).

¹⁰R. Heitz, M. Veit, N. N. Ledentsov, A. Hoffmann, D. Bimberg, V. M. Ustinov, P. S. Kop'ev, and Zh. I. Alferov, *Phys. Rev. B* **56**, 10 435 (1997).

¹¹P. W. Fry, I. E. Itskevich, D. J. Mowbray, M. S. Skolnick, J. J. Finley, J. A. Barker, E. P. O'Reilly, L. R. Wilson, I. A. Larkin, P. A. Maksym, M. Hopkinson, M. Al-Khafaji, J. P. R. David, A. G. Cullis, G. Hill, and J. C. Clark, *Phys. Rev. Lett.* **84**, 733 (2000).

¹²P. W. Fry, J. J. Finley, L. R. Wilson, A. Lemaitre, D. J. Mowbray, M. S. Skolnick, M. Hopkinson, G. Hill, and J. C. Clark, *Appl. Phys. Lett.* **77**, 4344 (2000).

¹³W.-H. Chang, T. M. Hsu, C. C. Huang, S. L. Hsu, C. Y. Lai, N. T. Yeh, T. E. Nee, and J.-I. Chyi, *Phys. Rev. B* **62**, 6959 (2000).

¹⁴J. Kim, L.-W. Wang, and A. Zunger, *Phys. Rev. B* **57**, R9408 (1998); A. J. Williamson, L. W. Wang, and Alex Zunger, *ibid.* **62**, 12 963 (2000).

¹⁵O. Stier, M. Grundmann, and D. Bimberg, *Phys. Rev. B* **59**, 5688 (1999).

¹⁶A. Patanè, A. Levin, A. Polimeni, P. C. Main, L. Eaves, M. Henini, and G. Hill, *Phys. Rev. B* **62**, 11 084 (2000).

¹⁷S. C. McFarlane, J. Barnes, K. W. J. Barnham, E. S. M. Tsui, C. Button, and J. S. Roberts, *J. Appl. Phys.* **86**, 5109 (1999).

¹⁸E. H. Nicollian and A. Goetzberger, *Bell Syst. Tech. J.* **46**, 1055 (1967).

¹⁹C. M. A. Kapteyn, F. Heinrichsdorff, O. Stier, R. Heitz, M. Grundmann, N. D. Zakharov, D. Bimberg, and P. Werner, *Phys. Rev. B* **60**, 14 265 (1999).

²⁰F. Findeis, M. Baier, E. Beham, A. Zrenner, and G. Abstreiter, *Appl. Phys. Lett.* **78**, 2958 (2001).